ICSV13 - Vienna
The Thirteenth International Congress on Sound and Vibration
Vienna, Austria, July 2-6, 2006

A THIN ORTHOTROPIC PLATE UNDER TRANSVERSE IMPULSE LOADING

Jan Cerv*, Frantisek Vales and Jan Volek

Institute of Thermomechanics AS CR, Department of Impact and Waves in Solids,
Dolejskova 5, 182 00 Prague 8, Czech Republic
cerv@it.cas.cz

Abstract

Analytical solutions based on Flügge and Mindlin approximations of a thin elastic orthotropic plate under transverse impulse loading are discussed in the paper. The loading is supposed to be given as an arbitrary function of space and time. The results in the form of displacements and velocities are compared with those obtained by 3D finite element solution. Dispersion behaviour of the Mindlin approximation of a thin elastic orthotropic plate is studied as well. It was found out that there are allways three different dispersion curves for any arbitrary direction of propagation.

INTRODUCTION

Thin-walled structures can be modelled and simulated with the help of the three-dimensional continuum mechanics. In this case the analytical and numerical effort is high, and the accuracy of the results is in some cases not adequate to the increase of the hard work. This and other difficulties are the reason for developing various approximative theories for plates and other thin-walled structural elements during the last 200 years. The paper is devoted to the fundamentals and some improvements of the classical plate theory proposed by Kirchhoff. It is known that any plate theory is an approximation of the three-dimensional theory and the approximations are always connected with some loss of information. Therefore the results obtained in this paper via approximative theories have been compared with those obtained by 3D finite element solution. In this research four analytical models were used for the description of thin plate behaviour. In the first of them (known as Kirchhoff model) the plate is assumed to be under a state of pure bending in which plane sections of the plate remain plane and perpendicular to the midplane of the plate. Thus, shear deformation is not included in this model. A state of plane stress is also supposed and the effects

of rotatory inertia are neglected. In the second model (known as Rayleigh model) the effects of rotatory inertia are also included without any shear deformation. Third model (known as Flügge model) incorporates shear deformations but no rotatory inertia effects. Fourth model (known as Mindlin model) takes into account (against Kirchhoff model) both rotatory inertia effects and shear deformations.

PROBLEM FORMULATION

The scheme of the problem solved is illustrated in Fig.1. The transverse pressure loading $p(x,y,t)$, with the resulting force F_0 , is distributed over a small circle having $2c$ diameter and center (x_F , y_F). This loading is applied to the upper face of a thin elastic bounded plate a x b x h , where h is the thickness. The lower plate face is traction-free.

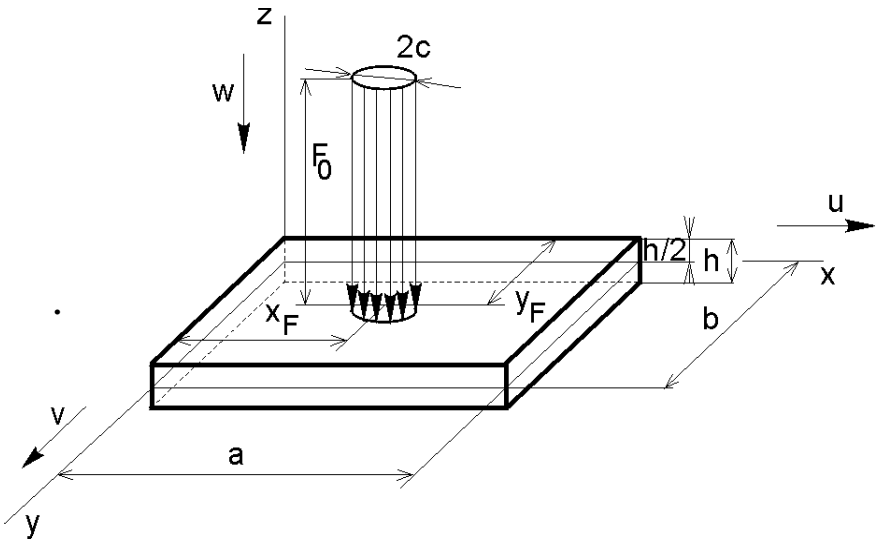

Figure 1 - Model under study

The time and space dependence of the loading may be given by an arbitrary function. The plate material is supposed to be linear elastic, homogeneous and orthotropic. Principal material and body axes coincide. At the beginning the plate is at rest (zero initial conditions) and without any stress. Displacements in the directions of axes x, y, z are denoted by u, v, w respectively. Material density is given by ρ.

THEORY

For the sake of brevity we will concentrate here on Flügge and Mindlin models only. The results obtained by Kirchhoff and also Rayleigh approximations are at the disposal as well and will be presented at the oral presentation.

Kinematics, plate stress-displacement relations and equations of motion for Flügge and Mindlin models

The total slope of any element of the plate consists of a rotation due to pure bending and a rotation due to shear strain γ (at z = 0) and so we have for small deflections $w(x,y,t)$, bending slopes $\varphi_x(x,y,t)$, $\varphi_y(x,y,t)$ and shear strain γ_{xz} , γ_{yz}

$$\frac{\partial w}{\partial x} = \varphi_x + \gamma_{xz}\,,\ \ \frac{\partial w}{\partial y} = \varphi_y + \gamma_{yz}\,,\ \ u(x,y,z,t) = -z\cdot\varphi_x\,,\ \ v(x,y,z,t) = -z\cdot\varphi_y\,. \tag{1}$$

The stresses are given from general Hooke's law as

$$\sigma_x = \frac{-zE_x}{1-\mu_{xy}\mu_{yx}}\left(\frac{\partial\varphi_x}{\partial x} + \mu_{yx}\frac{\partial\varphi_y}{\partial y}\right), \qquad \sigma_y = \frac{-zE_y}{1-\mu_{xy}\mu_{yx}}\left(\frac{\partial\varphi_y}{\partial y} + \mu_{xy}\frac{\partial\varphi_x}{\partial x}\right),$$
$$\tau_{xy} = -z\cdot G_{xy}\left(\frac{\partial\varphi_x}{\partial y} + \frac{\partial\varphi_y}{\partial x}\right),\ \tau_{yz} = G_{yz}\left(\frac{\partial w}{\partial y} - \varphi_y\right),\ \tau_{xz} = G_{xz}\left(\frac{\partial w}{\partial x} - \varphi_x\right)\,. \tag{2}$$

Denoting k_x (and similarly k_y) the ratio of average shear stress τ_{xz} (τ_{yz}) to the max(τ_{xz}) (max(τ_{yz})) across the plate thickness (τ_{xz} and τ_{yz} are distributed parabolically here), we can write the equations of motion for the both models. So we obtain for the **Flügge** model the following system

$$\begin{aligned}
&\frac{\partial^2 w}{\partial t^2} - \frac{G_{xz}k_x}{\rho}\frac{\partial^2 w}{\partial x^2} - \frac{G_{yz}k_y}{\rho}\frac{\partial^2 w}{\partial y^2} + \frac{G_{xz}k_x}{\rho}\frac{\partial\varphi_x}{\partial x} + \frac{G_{yz}k_y}{\rho}\frac{\partial\varphi_y}{\partial y} = \frac{p(x,y,t)}{\rho h}\,,\\
&-\frac{12G_{yz}k_y}{\rho h^2}\frac{\partial w}{\partial y} - \frac{12(D_{xy}+\mu_{xy}D_y)}{\rho h^3}\frac{\partial^2\varphi_x}{\partial x\partial y} - \frac{12D_{xy}}{\rho h^3}\frac{\partial^2\varphi_y}{\partial x^2} - \frac{12D_y}{\rho h^3}\frac{\partial^2\varphi_y}{\partial y^2} + \frac{12G_{yz}k_y}{\rho h^2}\varphi_y = 0\,,\\
&-\frac{12G_{xz}k_x}{\rho h^2}\frac{\partial w}{\partial x} - \frac{12(D_{xy}+\mu_{yx}D_x)}{\rho h^3}\frac{\partial^2\varphi_y}{\partial x\partial y} - \frac{12D_{xy}}{\rho h^3}\frac{\partial^2\varphi_x}{\partial y^2} - \frac{12D_x}{\rho h^3}\frac{\partial^2\varphi_x}{\partial x^2} + \frac{12G_{xz}k_x}{\rho h^2}\varphi_x = 0\,.
\end{aligned} \tag{3}$$

For the **Mindlin** model the system of equations of motion has the form

$$\begin{aligned}
&\frac{\partial^2 w}{\partial t^2} - \frac{G_{xz}k_x}{\rho}\frac{\partial^2 w}{\partial x^2} - \frac{G_{yz}k_y}{\rho}\frac{\partial^2 w}{\partial y^2} + \frac{G_{xz}k_x}{\rho}\frac{\partial\varphi_x}{\partial x} + \frac{G_{yz}k_y}{\rho}\frac{\partial\varphi_y}{\partial y} = \frac{p(x,y,t)}{\rho h}\,,\\
&\frac{\partial^2\varphi_y}{\partial t^2} - \frac{12G_{yz}k_y}{\rho h^2}\frac{\partial w}{\partial y} - \frac{12(D_{xy}+\mu_{xy}D_y)}{\rho h^3}\frac{\partial^2\varphi_x}{\partial x\partial y} - \frac{12D_{xy}}{\rho h^3}\frac{\partial^2\varphi_y}{\partial x^2} - \frac{12D_y}{\rho h^3}\frac{\partial^2\varphi_y}{\partial y^2} + \frac{12G_{yz}k_y}{\rho h^2}\varphi_y = 0,\\
&\frac{\partial^2\varphi_x}{\partial t^2} - \frac{12G_{xz}k_x}{\rho h^2}\frac{\partial w}{\partial x} - \frac{12(D_{xy}+\mu_{yx}D_x)}{\rho h^3}\frac{\partial^2\varphi_y}{\partial x\partial y} - \frac{12D_{xy}}{\rho h^3}\frac{\partial^2\varphi_x}{\partial y^2} - \frac{12D_x}{\rho h^3}\frac{\partial^2\varphi_x}{\partial x^2} + \frac{12G_{xz}k_x}{\rho h^2}\varphi_x = 0.
\end{aligned} \tag{4}$$

For D_x, D_y, D_{xy} in (3) and (4) we have

$$D_x = \frac{E_x h^3}{12(1-\mu_{xy}\mu_{yx})}, \quad D_y = \frac{E_y h^3}{12(1-\mu_{xy}\mu_{yx})}, \quad D_{xy} = \frac{G_{xy} h^3}{12}. \tag{5}$$

Shear stresses τ_{xz}, τ_{yz} for all the considered models have the parabolical dependence on the coordinate z.

SOLUTION

As an example we outline the solution of rectangular Mindlin plate having simply supported edges, see Fig.1. In this case we may assume the solution of the system (4) in the form

$$\begin{aligned} w(x,y,t) &= \sum_{m=1}^{\infty}\sum_{n=1}^{\infty} W(t)\sin(\alpha_m x)\sin(\beta_n y), \\ \varphi_x(x,y,t) &= \sum_{m=1}^{\infty}\sum_{n=1}^{\infty} FX(t)\cos(\alpha_m x)\sin(\beta_n y), \\ \varphi_y(x,y,t) &= \sum_{m=1}^{\infty}\sum_{n=1}^{\infty} FY(t)\sin(\alpha_m x)\cos(\beta_n y), \end{aligned} \tag{6}$$

where $\alpha_m = \frac{m\pi}{a}$, $\beta_n = \frac{n\pi}{b}$. The functions W and FX, FY represent time dependences of displacement w and slopes φ_x, φ_y respectively. Substituting from (6) into Eqs. (4) we obtain, after some lengthy manipulations, the following set of equations for W, FX, FY

$$\begin{aligned} &\frac{d^2W(t)}{dt^2} + (a1\alpha_m^2 + a2\beta_n^2)W(t) - a1\alpha_m FX(t) - a2\beta_n FY(t) = F(t), \\ &\frac{d^2FX(t)}{dt^2} - a7\alpha_m W(t) + (a9\alpha_m^2 + a5\beta_n^2 + a7)FX(t) + a8\alpha_m\beta_n FY(t) = 0, \\ &\frac{d^2FY(t)}{dt^2} - a3\beta_n W(t) + a4\alpha_m\beta_n FX(t) + (a5\alpha_m^2 + a6\beta_n^2 + a3)FY(t) = 0, \end{aligned} \tag{7}$$

where

$$F(t) = \frac{4}{\rho h a b}\int_0^a\int_0^b p(x,y,t)\sin(\alpha_m x)\sin(\beta_n y)dxdy. \tag{8}$$

For a1,a2,a3,..... a9 in set (7), it holds

$$a1=\frac{G_{xz}k_x}{\rho}\ ,\ a2=\frac{G_{yz}k_y}{\rho}\ ,\ a3=\frac{12G_{yz}k_y}{\rho h^2}\ ,\ a4=\frac{G_{xy}}{\rho}+\frac{\mu_{xy}E_y}{\rho(1-\mu_{xy}\mu_{yx})}\ ,\ a5=\frac{G_{xy}}{\rho}\ ,$$
$$a6=\frac{E_y}{\rho(1-\mu_{xy}\mu_{yx})}\ ,\ a7=\frac{12G_{xz}k_x}{\rho h^2}\ ,\ a8=\frac{G_{xy}}{\rho}+\frac{\mu_{yx}E_x}{\rho(1-\mu_{xy}\mu_{yx})}\ ,\ a9=\frac{E_x}{\rho(1-\mu_{xy}\mu_{yx})}\ . \tag{9}$$

Applying the Laplace transform to system (7) and considering the zero initial conditions, we obtain the set of three equations for transformed functions $\overline{W}(s),\overline{FX}(s),\overline{FY}(s)$, where s is the Laplace transform parameter. The solution particular images $\overline{W}(s),\overline{FX}(s),\overline{FY}(s)$ and then the Laplace inversion leads to following relations for looked-for functions *W, FX, FY.* So we have

$$W(t)=\sum_{j=1}^{3}\frac{Wj}{\omega_j}\int_0^t F(\tau)\sin\left[\omega_j(t-\tau)\right]d\tau\,,$$
$$FX(t)=\sum_{j=1}^{3}\frac{Xj}{\omega_j}\int_0^t F(\tau)\sin\left[\omega_j(t-\tau)\right]d\tau\,,$$
$$FY(t)=\sum_{j=1}^{3}\frac{Yj}{\omega_j}\int_0^t F(\tau)\sin\left[\omega_j(t-\tau)\right]d\tau\,, \tag{10}$$

where W_j , X_j and Y_j are somewhat complicated function obtained in the course of the solution by Laplace transform and ω_j are roots of some bicubical equation. For brevity, their forms are not shown here. Substituting (10) into (6) gives the resulting expressions for w, φ_x , φ_y . For the specified load shown in Fig.1, having Heaviside (step) time dependence, the results may be written in the form

$$w(x,y,t)=\frac{16F_0}{\rho habc}\sum_{m=1}^{\infty}\sum_{n=1}^{\infty}\frac{J_1(\gamma_{mn}c)}{\gamma_{mn}}\sin(\alpha_m x)\sin(\beta_n y)\sin(\alpha_m x_F)\sin(\beta_n y_F)\sum_{j=1}^{3}\frac{Wj}{\omega_j^2}\sin^2(\frac{\omega_j t}{2}),$$

$$\varphi_x(x,y,t)=\frac{16F_0}{\rho habc}\sum_{m=1}^{\infty}\sum_{n=1}^{\infty}\frac{J_1(\gamma_{mn}c)}{\gamma_{mn}}\sin(\alpha_m x)\sin(\beta_n y)\cos(\alpha_m x_F)\sin(\beta_n y_F)\sum_{j=1}^{3}\frac{Xj}{\omega_j^2}\sin^2(\frac{\omega_j t}{2}),$$

$$\varphi_y(x,y,t)=\frac{16F_0}{\rho habc}\sum_{m=1}^{\infty}\sum_{n=1}^{\infty}\frac{J_1(\gamma_{mn}c)}{\gamma_{mn}}\sin(\alpha_m x)\sin(\beta_n y)\sin(\alpha_m x_F)\cos(\beta_n y_F)\sum_{j=1}^{3}\frac{Yj}{\omega_j^2}\sin^2(\frac{\omega_j t}{2}), \tag{11}$$

where $\gamma_{mn}=\sqrt{\left(\alpha_m^2+\beta_n^2\right)}$ and J_1 is the Bessel function of the first kind of order 1.

RESULTS

In all the analytic results shown here it is supposed that a square plate is made of orthotropic material of thickness $h=0.5\ mm$, $a = b = 60\ mm$. All analytic calculations were performed for $m = n = 1000$ normal modes, see Eqs.11. FE modelling of a wave motion in a plate was carried out by using the finite element code MARC 2005. A square plate $200 \times 200 \times 0.5\ mm$ was divided across the thickness into three same layers. Due to symmetry only a quarter of the plate has been modelled. So the sandwich plate $100 \times 100 \times 0.5\ mm$ was discretized by a grid of *121338* eight node brick elements. In the vicinity of the load the mesh was locally refined. The lumped mass matrix and the central difference scheme for the time integration were employed because errors in the temporal and spatial approximations tend to cancel each other. For FE calculations, the stability time step used was $0.004\mu s$.

A unidirectional material (Glass-epoxy) of the plate was assumed to be transversely isotropic (nine nonzero elastic stiffness moduli, five of which are independent), x axis was along the fibres, y axis was normal to the fibres and z axis was perpendicular to the plane of the plate, see Fig.1. The pressure with the resulting force $F_0 = 1N$ was distributed in the middle of the plate over the circular area of diameter 2c = 0.5 mm and has the Heaviside step time dependence. The mass density $\rho = 1800\ kg/m^3$. We introduce new variables ξ and η as distances from the load axis in the directions of x and y axes respectively. So we have $\xi = x - x_F$, $\eta = y - y_F$ and now we can compare the analytic results with those obtained by FE approach.

Elastic stiffness moduli are: $E_x = 38.6\ GPa$, $E_y = E_z = 8.27\ GPa$, $G_{yz} = 3.45\ GPa$, $G_{xz} = G_{xy} = 4.14\ GPa$, $\mu_{yz} = \mu_{xy} = 0.2$, $\mu_{xz} = 0.043$.

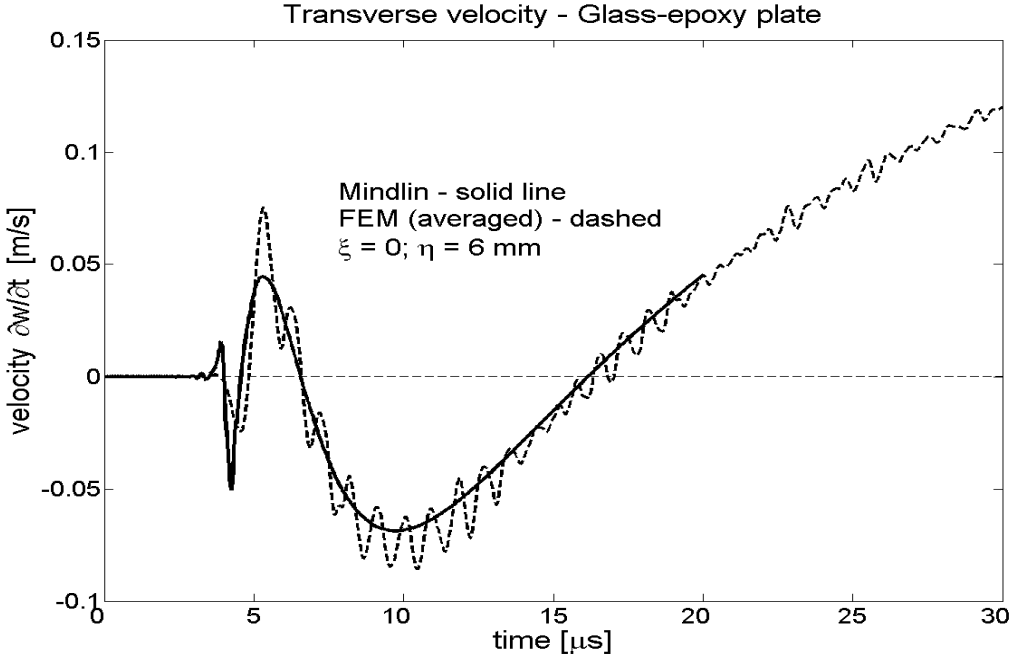

Fig.2 Transverse velocity time histories resulting from FEM (3D) and Mindlin models

In Fig.2, the transverse velocity time histories from both approaches at propagation distance $\xi = 0$, $\eta = 6$ *mm* are shown. FE values from top and bottom plate faces were averaged. It is seen that agreement between the two methods is quite good. It is the opinion of the authors, that some discrepancy between the two methods is given by approximative nature of Mindlin model. The Mindlin model cannot handle wave reflections from top and bottom plate faces.

Dispersion behaviour of Mindlin model

Let us consider an orthotropic plate, having thickness h as in Fig.1, but now of infinite extent in the x and y directions. We assume the following forms for deflections $w(x,y,t)$ and bending slopes $\varphi_x(x,y,t)$, $\varphi_y(x,y,t)$

$$w = W_0 \cdot \exp\left[ik\left(x\cos\alpha + y\sin\alpha - ct\right)\right],\ \varphi_x = \Phi_x \cdot \exp\left[ik\left(x\cos\alpha + y\sin\alpha - ct\right) + i\cdot\Theta_x\right],$$
$$\varphi_y = \Phi_y \cdot \exp\left[ik\left(x\cos\alpha + y\sin\alpha - ct\right) + i\cdot\Theta_y\right], \tag{12}$$

where W_0 , Φ_x , Φ_y are the amplitudes, k is the wavenumber, c is the phase velocity and $cos\alpha$, $sin\alpha$ are the x,y components of the unit wave vector respectively. Θ_x and Θ_y are the corresponding phase angles.

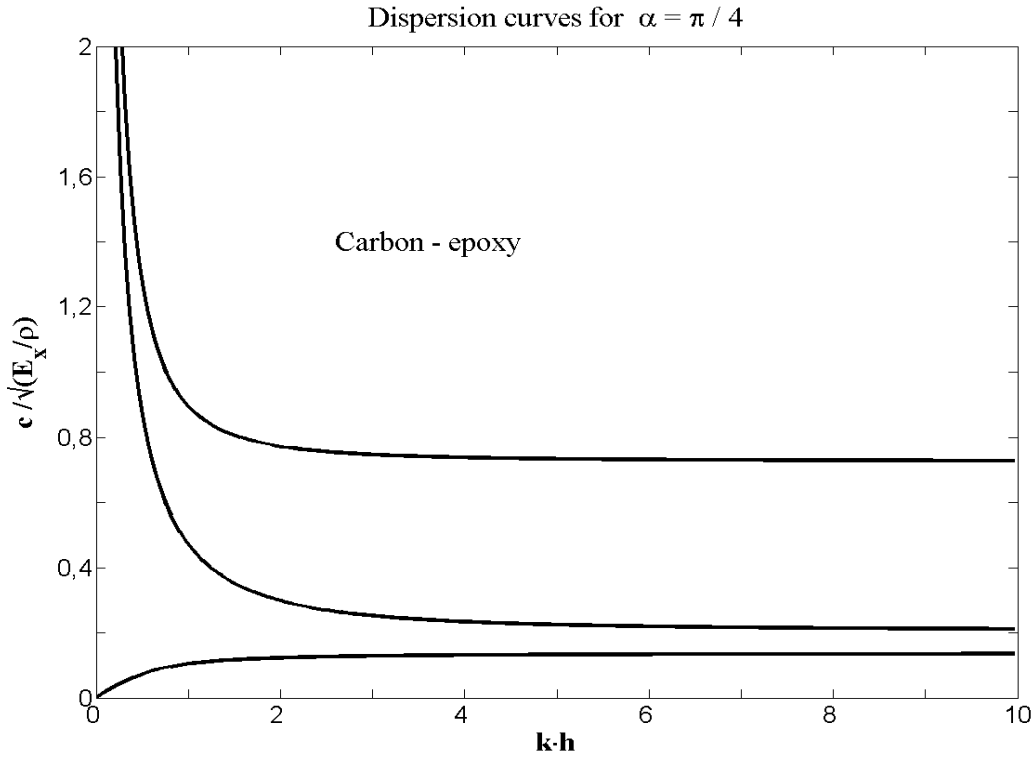

Fig.3 Dispersion curves for Mindlin model ($\alpha = \pi / 4$))

Substituting (12) into homogeneous (loading $p(x,y,t) = 0$) equations of motion (4) we get after some algebra $\Theta_x = \Theta_y = \pi/2$ and also the homogeneous set for W_0 , Φ_x , Φ_y . For nontrivial solution, we obtain the characteristic bicubic equation for the dimensionless velocity $c/\sqrt{\frac{E_x}{\rho}}$. Numerical solutions of the characteristic equation yield for every direction of propagation three dispersion curves. The curves describe the dependence of the dimensionless velocity on dimensionless wavenumber *kh*. The Fig.3 illustrates the dispersion curves for the direction of propagation $\alpha = \pi/4$. The plate is made of Carbon-epoxy with the following material constants: $E_x = 142.2$ *GPa,* $E_y = E_z = 9.255$ *GPa,* $G_{yz} = 3.114$ *GPa,* $G_{xz} = G_{xy} = 4.795$ *GPa,* $\mu_{xz} = \mu_{xy} = 0.334$, $\mu_{yz} = 0.486$, $\rho = 1900\ kg/m^3$.

SUMMARY

The solutions based on Flügge and Mindlin approximations of a thin elastic orthotropic plate under transverse impulse loading are discussed in the paper. The results in the form of displacements and velocities are compared with those obtained by 3D finite element solution. Dispersion behaviour of the Mindlin approximation is studied as well. It was found out that there are allways three different dispersion curves for any arbitrary direction of propagation. The influence of the shear correction factors k_x , k_y on the dispersion was investigated by the authors and many others [1]. Dispersion curves were found to be fairly insensitive to the above factors. Effects of viscoelasticity on thin plate behaviour were investigated in [2].

ACKNOWLEDGEMENT

The work was supported by the grant agencies GA AS CR and GA CR under contracts No. **A200760611** , **101/06/0213**.

REFERENCES

[1] S. Vlachoutsis, "Shear correction factors for plates and shells", International Journal for Numerical Methods in Engineering , **33**, no. 7, 1537-1552 (1992)

[2] V.Adamek, F.Vales and V.Las, "Analytical and numerical solution of non-stationary state of stress in a thin viscoelastic plate", Nonlinear Analysis, **63**, e955-e962 (2005)